International Journal of Thermophysics, Vol. 16, No. 4, 1995

Thermophysical Properties of *m*-Cresol as a Function of Temperture (303 to 503 K) and Pressure (0.1 to 400 MPa)

S. L. Randzio,[1] E. A. Lewis,[2] D. J. Eatough,[2] and L. D. Hansen[2,3]

Received September 23, 1994

Measured and derived thermophysical properties of *m*-cresol are reported for pressures up to 400 MPa at temperatures from 303 to 503 K. Isobaric thermal expansivities were measured by pressure-scanning calorimetry from 303 to 503 K and 0.1 to 400 MPa. The specific volume at 353 K was determined by pycnometry at atmospheric pressure and calculated from isothermal compressibilities measured as a funtion of pressure up to 400 MPa. Specific volumes at other temperatures and pressures are calculated from isothermal compressibilities measured as a function of pressure up to 400 MPa. Specific volumes, isothermal compressibilities, thermal coefficients of pressure, and isobaric and isochoric heat capacities at pressures up to 400 MPa are derived at several temperatures. The effects of pressure on the isobaric heat capacities of *m*-cresol, *n*-hexane, and water are compared. The effects of self-association of *m*-cresol are apparent in both the thermal expansivity and the heat capacity data.

KEY WORDS: heat capacity; isobaric thermal expansivity; isothermal compressibility; *m*-cresol; pressure-scanning calorimetry; specific volume; thermal coefficient of pressure.

1. INTRODUCTION

As part of an effort to establish sets of reliable thermophysical data for various liquids over large ranges of temperature and pressure, the present paper reports data for liquid *m*-cresol, a self-associated liquid. A previous

[1] Institute of Physical Chemistry, Polish Academy of Sciences, ul. Kasprazaka 44/52, 01-224 Warsaw, Poland.
[2] Department of Chemistry, Brigham Young University, Provo, Utah 84602, U.S.A.
[3] To whom correspondence should be addressed.

840/16/4-3

paper [1] presented data for *n*-hexane, an example of a liquid without strong specific intermolecular interactions. The self-association and hydrogen bonding of *m*-cresol with Lewis bases have been widely studied [2–10]. *m*-Cresol is also of theoretical interest because of rotational isomerism arising from orientation of the OH group with respect to the CH_3 group at the meta position [11, 12]. Temperature was the intensive variable in these previous studies, and thus the thermodynamic analysis was limited to temperature derivatives of the thermodynamic functions. The effects of pressure on the properties of *m*-cresol are unknown except for measurements of the enthalpy of *m*-cresol up to a few megapascals [9], a pressure range too small for accurate determination of the pressure derivatives of thermodynamic functions.

The present paper presents results of measurements of isobaric thermal expansivity from 303 to 503 K and from 0.1 to 400 MPa and of the specific volume of *m*-cresol as a function of pressure at 353.15 K. Specific volumes, isothermal compressibilities, and isobaric and isochoric heat capacities for the pressure range up to 400 MPa at selected temperatures from 353.15 to 503.15 K are derived from these data and from literature data on the isobaric heat capacity at atmospheric pressure. The influence of pressure on the heat capacity of *m*-cresol is emphasized in the present study. Pressure derivatives of the isobaric heat capacities of *m*-cresol, *n*-hexane and water are compared.

2. EXPERIMENTS

Measurements of thermal expansivities were made with a stepwise pressure-scanning calorimeter previously described [13]. Calorimetric determination of thermal expansivity is based on the following equation [13, 14]:

$$\alpha_p - \alpha_{p,ss} = -kI/(T\,\Delta p) \tag{1}$$

where k ($\mathrm{MPa \cdot V^{-1} \cdot s^{-1}}$) is the instrument calibration constant at various temperatures as given in a previous paper [13], I ($\mathrm{V \cdot s}$) is the time integral of the calorimetric signal (heat rate) resulting from the calorimeter response to a pressure step Δp (MPa), $\alpha_{p,ss}$ ($5.1 \times 10^{-5}\ \mathrm{K^{-1}}$) is the thermal expansivity of the stainless-steel calorimeter cell, and T (K) is the absolute temperature.

To prevent sorption of moisture, the *m*-cresol was kept under argon, transferred with a syringe, and immediately injected into the calorimetric vessel, which was rapidly closed with a cone and cone-retaining gland in such a way that no vapor space was present. After pressurizing to the highest pressure, the system was allowed to equilibrate thermally and mechanically

for a few hours before measurements began. Measurements were made with decreasing pressure.

The volume of *m*-cresol as a function of pressure at 353.15 K was determined by a previously described method [13] with the automated, stepper-motor driven, pressure generating system of the pressure-scanning calorimeter in Warsaw [15]. The rate of external volume change was kept small ($\approx 1 \times 10^{-4}$ cm$^3 \cdot$ s^{-1}) so as to make the effect of compression heating negligible. Also, the program was occasionally stopped to make certain the measuring system was at thermal equilibrium. Calibration of the pressure generating system for compressibility measurements was done with *n*-hexane. The specific volume of *n*-hexane over the pressure and temperature range used in this study is known better than $\pm 0.2\%$ [1]. The static calibration constant obtained was $(5.838 \pm 0.014) \times 10^{-6}$ cm^3 per motor step. This calibration constant depends only on temperature. A more detailed description of the calibration procedure for compressibility measurements is given in Ref. 16. Full-scale resolution in the compressibility measurements was ± 2 ppm.

The specific volume of *m*-cresol at 353.15 K at atmospheric pressure was measured to $\pm 0.2\%$ with a pycnometer calibrated with water. The *m*-cresol used in this study without further purification was Aldrich Gold Label, No. C8572-7, 99+%.

3. RESULTS

3.1. Isobaric Cofficient of Thermal Expansion, α_p

Isobaric thermal expansivities measured at 303.15, 353.15, 403.15, 453.15, and 503.15 K are given in Table I. Pressure values given in Table I are the mean of the pressures at the beginning and end of a pressure step. The end values were measured at the end of the thermogram, after thermal and mechanical equilibrium was reestablished. Each ending pressure became the beginning pressure for the next step. The isothermal solid–liquid transition was observed at 303.15 K as large changes in α_p values above about 90 MPa. Values of α_p obtained with both phases present are equal to the weighted sum of the thermal expansivities of solid and liquid and the entropy change due to the phase transition. The entropy change is the largest term. Available data are insufficient for further analysis.

The accuracy limits given in Table I are the estimated maximal errors determined from uncertainties in the measured pressures (± 0.14 MPa), integrals [I in Eq. (1), $\pm 0.2\%$], temperature (± 0.1 K), $\alpha_{p,ss}$ ($\pm 10\%$), and calibration constant (k in Eq. (1)), from ± 0.4 to 1.7%, depending on temperature [13]).

Table I. Results of Pressure-Scanning Calorimetric Measurements of Isobaric Thermal Expansivity of *m*-Cresol

p (MPa)	Δp (MPa)[a]	α_p (10^{-4} K^{-1})	p (MPa)	Δp (MPa)[a]	α_p (10^{-4} K^{-1})
		$T = 303.15$ K			
350.4	19.24	2.72 ± 0.09	156.6	13.58	29.20 ± 0.87
327.3	27.01	3.05 ± 0.09	142.7	14.20	60.20 ± 1.75
299.1	29.30	3.65 ± 0.11	133.2	4.62	117.00 ± 5.81
271.7	25.37	4.29 ± 0.13	117.2	32.31	32.80 ± 0.78
245.8	26.54	5.34 ± 0.13	89.2	28.89	6.70 ± 0.16
219.0	27.03	7.08 ± 0.17	60.7	28.13	6.50 ± 0.16
193.7	23.51	10.60 ± 0.27	31.9	29.37	7.01 ± 0.17
172.7	18.55	17.70 ± 0.48	9.3	15.86	7.55 ± 0.21
		$T = 353.15$ K			
330.3	16.39	4.54 ± 0.11	128.2	24.13	5.96 ± 0.11
309.1	26.13	4.62 ± 0.08	104.4	23.51	6.25 ± 0.11
281.8	28.34	4.79 ± 0.08	82.4	20.48	6.67 ± 0.13
254.2	26.89	4.87 ± 0.08	62.3	19.65	6.90 ± 0.14
228.7	24.06	5.08 ± 0.09	42.8	19.31	7.36 ± 0.15
203.3	26.75	5.23 ± 0.09	24.4	17.31	7.94 ± 0.18
177.4	25.03	5.47 ± 0.09	8.8	14.00	8.27 ± 0.22
152.6	24.68	5.76 ± 0.10			
		$T = 403.15$ K			
352.3	16.00	4.31 ± 0.10	144.8	21.44	6.00 ± 0.12
332.8	19.10	4.48 ± 0.09	123.3	21.58	6.23 ± 0.12
311.4	23.65	4.47 ± 0.08	100.7	23.58	6.53 ± 0.12
286.9	25.37	4.68 ± 0.08	78.2	21.44	7.03 ± 0.14
261.3	25.86	4.91 ± 0.08	56.0	23.10	7.48 ± 0.14
212.5	23.17	5.35 ± 0.10	33.4	15.86	8.16 ± 0.20
189.7	22.34	5.49 ± 0.10	19.0	13.10	8.96 ± 0.25
167.1	23.03	5.71 ± 0.11	6.7	11.45	9.18 ± 0.28
		$T = 453.15$ K			
350.5	19.03	4.39 ± 0.12	162.7	21.44	5.91 ± 0.15
330.4	21.17	4.34 ± 0.11	140.6	22.82	6.05 ± 0.15
309.4	20.89	4.52 ± 0.12	117.9	22.41	6.10 ± 0.15
285.8	26.20	4.64 ± 0.11	97.0	21.58	6.66 ± 0.17
260.1	25.23	4.82 ± 0.11	72.4	27.58	7.40 ± 0.17
234.8	25.23	4.91 ± 0.12	47.4	22.34	8.05 ± 0.20
210.9	22.61	5.08 ± 0.13	27.4	17.65	8.60 ± 0.24
186.5	26.20	5.35 ± 0.12	10.0	17.31	9.73 ± 0.27
		$T = 503.15$ K			
349.5	18.06	4.29 ± 0.14	139.9	23.58	5.91 ± 0.17
283.7	21.37	4.34 ± 0.13	115.2	24.48	6.14 ± 0.15
260.9	24.27	4.59 ± 0.13	92.2	22.96	6.65 ± 0.20
237.1	23.24	4.66 ± 0.14	69.0	23.30	7.41 ± 0.22
212.6	26.61	5.03 ± 0.14	27.6	17.93	9.21 ± 0.30
187.2	24.13	5.01 ± 0.14	10.0	17.24	10.00 ± 0.34
163.4	23.44	5.48 ± 0.16			

[a] See Eq. (1).

Table II. Values of Coefficients in Eqs. (3), (4), (7), and (12) for Liquid *m*-Cresol

Eq.	a_0	a_1	a_2	a_3
(3)	3.556×10^{-3} MPa$^{-1/2}$·K^{-1}	3.64594×10^{-5} MPa$^{-1/2}$·K^{-2}	-5.53935×10^{-8} MPa$^{-1/2}$·K^{-3}	—
(4)	337.7 MPa	−0.67058 MPa·K^{-1}	1.73836×10^{-4} MPa·K^{-2}	—
(7)	31.1133	−9926.49 K	−0.0353567 K^{-1}	1.90207×10^{-5} K^{-2}
(12)	−1.79244 kJ·K^{-1}·kg^{-1}	2.73642×10^{-2} kJ·K^{-2}·kg^{-1}	-6.32388×10^{-5} kJ·K^{-3}·kg^{-1}	5.17299×10^{-8} kJ·K^{-4}·kg^{-1}

The results with only liquid phase present were fitted by the least-squares method to Eqs. (2)–(4)

$$\alpha_p(p, T) = [a(T)][p + b(T)]^{-0.5} \tag{2}$$

where

$$a(T) = a_0 + a_1 T + a_2 T^2 \tag{3}$$

and

$$b(T) = a_0 + a_1 T + a_2 T^2 \tag{4}$$

with the resulting coefficients given in Table II, with pressure expressed as MPa. The standard deviation of the difference between an experimental

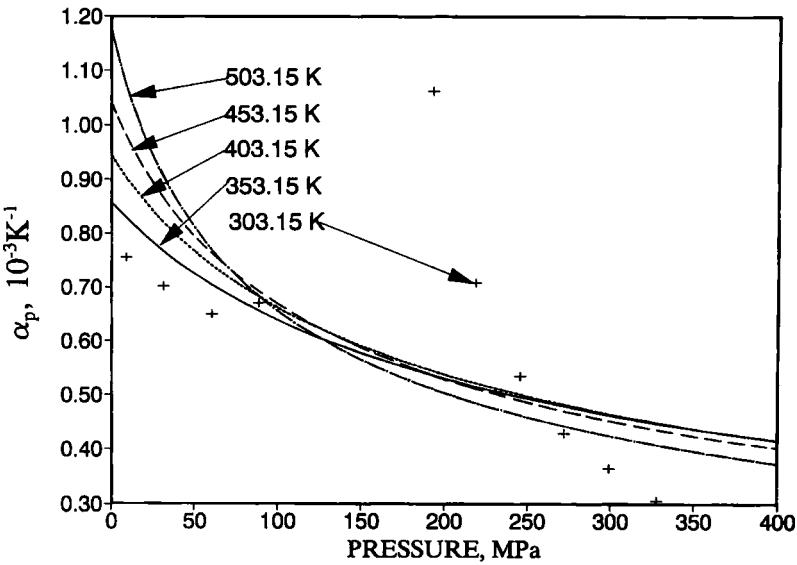

Fig. 1. Isobaric thermal expansivity (α_p) of *m*-cresol calculated with Eqs. (2)–(4) at 353.15 to 503.15 K and with Eq. (1) at 303.15 K.

data point and a value calculated from Eqs. (2)–(4) is ±2.0% with randomly distributed errors. Calculated α_p values at 353.15, 403.15, 453.15, and 503.15 K as well as the experimental data at 303.15 K are given in Fig. 1. The estimated error in the calculated α_p values is ±0.7%. There is no unique crossing point of the isotherms of the coefficient of isobaric thermal expansion as has been observed in several examples of liquids without strong intermolecular interactions [17]. However, the isotherms for *m*-cresol do cross and the crossing point moves to lower pressures as the temperature increases.

3.2. Specific Volume, $v(p, T)$

The specific volumes of liquid *m*-cresol at 353.15 K and various pressures are given in Table III, column 2. The data in column 2 are derived from pycnometric measurements at atmospheric pressure and compressibility measurements as a function of pressure. Note that experimental measurements were made only at 353.15 K. Equation (5) was fitted to the specific volume data at 353.15 K by least squares.

$$v(T_R, p) = v_0\{1 - C \ln[(B+p)/(B+0.1013)]\} \tag{5}$$

with p expressed as MPa, $v_0 = 1.0134\ \mathrm{cm^3 \cdot g^{-1}}$, $B = 108.399$, and $C = 0.0766197$. The standard deviation of the differences between the experimental data points and the values calculated from Eq. (5) is ±0.0033%, with the deviations being randomly distributed. $T_R = 353.15$ K was taken as the reference temperature and $v(T_R, p)$ as the reference volume isotherm for derivation of further thermodynamic quantities for the liquid phase of *m*-cresol.

The specific volumes of liquid *m*-cresol at temperatures above 353.15 K and from the saturated vapor pressure up to 400 MPa were obtained from Eq. (6) using thermal expansivities from Eqs. (2)–(4) and the specific volume isotherm at 353.15 K from Eq. (5).

$$v(p, T) = v(T_R, p) \exp\left[\int_{T_R}^{T} \alpha_p \, dT\right] \tag{6}$$

The saturation vapor pressure (p_s) from the normal boiling point, 475.35 K, to 503.15 K was obtained by the least-squares fit of Eq. (7) to vapor pressure data in Refs. 18–21.

$$p_s = \exp(a_0 + a_1 T^{-1} + a_2 T + a_3 T^2) \tag{7}$$

The coefficients giving p_s as MPa are given in Table II. Below the boiling point, specific volumes were calculated with 0.1013 MPa as the lower limit of integration. The results are given in Table III, columns 3–5.

Table III. Specific Volume ($1000\ m^3 \cdot kg^{-1}$) of Liquid *m*-Cresol

	T(K)			
p(MPa)	353.15	403.15	435.15	503.15
p_s	1.0134	1.0602	1.1141	1.1773
10	1.0066	1.0510	1.1015	1.1591
20	1.0003	1.0427	1.0901	1.1432
30	0.9945	1.0350	1.0799	1.1293
40	0.9891	1.0280	1.0707	1.1169
50	0.9840	1.0215	1.0622	1.1058
60	0.9793	1.0154	1.0544	1.0958
70	0.9748	1.0097	1.0472	1.0866
80	0.9706	1.0044	1.0405	1.0781
90	0.9665	0.9993	1.0342	1.0703
100	0.9627	0.9946	1.0283	1.0630
110	0.9591	0.9901	1.0227	1.0562
120	0.9556	0.9858	1.0175	1.0498
130	0.9523	0.9817	1.0125	1.0438
140	0.9491	0.9778	1.0078	1.0381
150	0.9460	0.9741	1.0033	1.0327
160	0.9431	0.9705	0.9990	1.0276
170	0.9402	0.9671	0.9949	1.0227
180	0.9375	0.9638	0.9910	1.0181
190	0.9348	0.9606	0.9872	1.0136
200	0.9323	0.9576	0.9836	1.0094
210	0.9298	0.9546	0.9801	1.0053
220	0.9274	0.9518	0.9767	1.0014
230	0.9251	0.9490	0.9735	0.9977
240	0.9228	0.9464	0.9704	0.9941
250	0.9206	0.9438	0.9673	0.9906
260	0.9185	0.9413	0.9644	0.9872
270	0.9164	0.9388	0.9616	0.9840
280	0.9144	0.9365	0.9588	0.9808
290	0.9124	0.9341	0.9562	0.9778
300	0.9105	0.9319	0.9536	0.9748
310	0.9086	0.9297	0.9511	0.9719
320	0.9068	0.9276	0.9486	0.9692
330	0.9050	0.9255	0.9463	0.9665
340	0.9032	0.9235	0.9439	0.9638
350	0.9015	0.9215	0.9417	0.9613
360	0.8998	0.9196	0.9395	0.9588
370	0.8982	0.9177	0.9373	0.9564
380	0.8966	0.9159	0.9352	0.9540
390	0.8950	0.9141	0.9332	0.9517
400	0.8935	0.9123	0.9312	0.9495

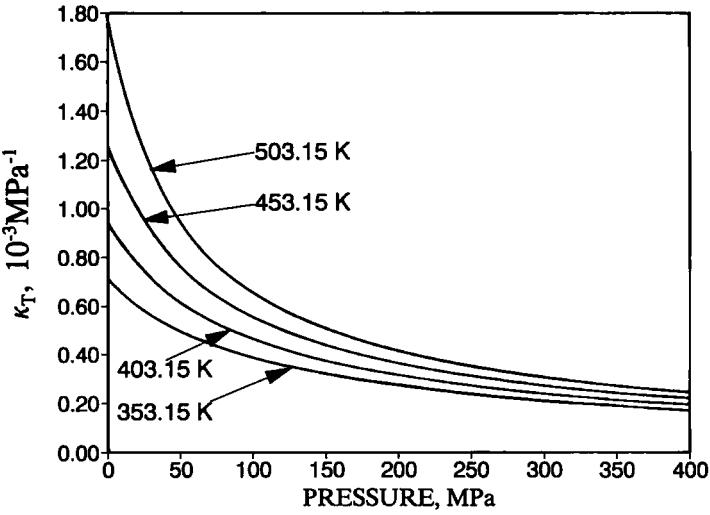

Fig. 2. Isothermal compressibility (κ_T) of liquid *m*-cresol calculated with Eq. (8).

3.3. Coefficient of Isothermal Compressibility, κ_T

Isothermal compressibilities were calculated with a form of the Tait equation, Eq. (8), at selected temperatures from 353.15 to 503.15 K at pressures from the saturated vapor pressure up to 400 MPa.

$$\kappa_T = C/\{(B+p)\{1 - C\ln[(B+p)/(B+p_s)]\}\} \tag{8}$$

Table IV gives the values of the coefficients B and C obtained by fitting the specific volume data in Table III. Table IV also gives standard and average deviations of the differences between the specific volumes derived with Eqs. (5) and (6) and the volumes obtained with the Tait equation at each

Table IV. Cofficients B and C of the Tait Equation, Eq. (8), for *m*-Cresol

T (K)	B (MPa)	C	SD (%)	Average deviation (%)
353.15	108.399	0.0766197	0.00	0.000
403.15	87.377	0.0813012	0.01	0.001
453.15	67.976	0.0853438	0.02	0.003
503.15	49.286	0.0879554	0.04	0.004

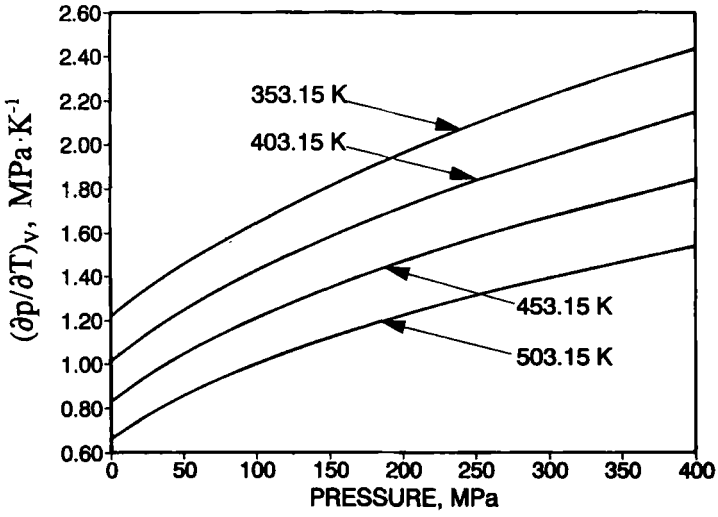

Fig. 3. Thermal coefficient of pressure $(\partial p/\partial T)_v$ of liquid *m*-cresol calculated with Eq. (9).

temperature. These error estimates are a good indication of the precision of the volume and compressibility data derived from the experimental data with Eqs. (5)–(7). A graphic presentation of isothermal compressibilities at selected temperatures is given in Fig. 2.

3.4. Thermal Coefficient of Pressure, $(\partial p/\partial T)_v$

The thermal coefficient of pressure of liquid *m*-cresol at selected temperatures from 353.15 to 503.15 K at pressures from the saturated vapor pressure up to 700 MPa was calculated with Eq. (9),

$$(\partial p/\partial T)_v = \alpha_p/\kappa_T \tag{9}$$

A graphic presentation of selected isotherms is given in Fig. 3. Numerical values for $(\partial p/\partial T)_v$ can be obtained from values for α_p from Eqs. (2)–(4) and values for κ_T from Eq. (8).

3.5. Isobaric Heat Capacity, $C_p^l(p, T)$

The effects of pressure on the isobaric heat capacity of liquid *m*-cresol at selected temperatures were calculated with Eq. (10).

$$\Delta_{p_s}^{p} C_{p,T}^{l}(p) = -T \int_{p_s}^{p} v(p, T)[\alpha^2 + (\partial \alpha_p/\partial T)_p]\, dp \tag{10}$$

Table V. Pressure Effects on the Isobaric Specific Heat Capacity of Liquid *m*-Cresol, $\Delta_{p_s}^{p} C_{p,T}^{l}(p)$, as $kJ \cdot K^{-1} \cdot kg^{-1}$

	T(K)			
p (MPa)	353.15	403.15	453.15	503.15
10	−0.008	−0.010	−0.014	−0.024
20	−0.015	−0.019	−0.026	−0.040
30	−0.022	−0.027	−0.035	−0.052
40	−0.028	−0.033	−0.042	−0.060
50	−0.033	−0.039	−0.048	−0.065
60	−0.038	−0.044	−0.052	−0.069
70	−0.043	−0.049	−0.056	−0.071
80	−0.047	−0.053	−0.059	−0.072
90	−0.051	−0.056	−0.062	−0.073
100	−0.054	−0.059	−0.064	−0.073
110	−0.057	−0.062	−0.066	−0.073
120	−0.061	−0.065	−0.067	−0.072
130	−0.063	−0.067	−0.068	−0.070
140	−0.066	−0.069	−0.069	−0.069
150	−0.069	−0.071	−0.070	−0.067
160	−0.071	−0.073	−0.070	−0.065
170	−0.074	−0.074	−0.070	−0.063
180	−0.076	−0.076	−0.070	−0.061
190	−0.078	−0.077	−0.070	−0.059
200	−0.080	−0.078	−0.070	−0.057
210	−0.082	−0.079	−0.070	−0.054
220	−0.083	−0.080	−0.069	−0.052
230	−0.085	−0.081	−0.069	−0.049
240	−0.087	−0.082	−0.068	−0.047
250	−0.088	−0.083	−0.068	−0.044
260	−0.090	−0.084	−0.067	−0.041
270	−0.091	−0.084	−0.066	−0.039
280	−0.093	−0.085	−0.066	−0.036
290	−0.094	−0.085	−0.065	−0.033
300	−0.095	−0.086	−0.064	−0.031
310	−0.096	−0.086	−0.063	−0.028
320	−0.098	−0.087	−0.062	−0.025
330	−0.099	−0.087	−0.061	−0.023
340	−0.100	−0.087	−0.060	−0.020
350	−0.101	−0.087	−0.059	−0.017
360	−0.102	−0.088	−0.058	−0.014
370	−0.103	−0.088	−0.057	−0.012
380	−0.104	−0.088	−0.056	−0.009
390	−0.105	−0.088	−0.055	−0.006
400	−0.106	−0.088	−0.054	−0.003

Values of $v(p, T)$ were calculated with Eqs. (5) and (6), α_p values with Eqs. (2)–(4), and $\partial\alpha_p/\partial T$ values with the derivative of Eqs. (2)–(4). $\Delta_{p_s}^{p} C_{p,T}^{l}(p)$ values were then obtained by numerical integration. The results of the calculations are given in Table V.

The isobaric heat capacity of liquid *m*-cresol as a function of p and T can be calculated with the thermodynamic relation in Eq. (11),

$$C_p^l(p, T) = C_{p,p_s}^l + \Delta_{p_s}^{p} C_p^l(p, T) \tag{11}$$

where C_{p,p_s}^l is the isobaric heat capacity of liquid *m*-cresol at the pressure of the saturated vapor. Direct experimental data for C_{p,p_s}^l are not available but can be calculated from literature data. Enthalphy data for *m*-cresol from Ref. 11 corrected for pressure effects were differentiated against temperature from 368.35 to 513.5 K. The values obtained together with data from Ref. 22 for heat capacities from 350 to 400 K were fitted by least squares to Eq. (12),

$$C_{p,p_s}^l(T) = a_0 + a_1 T + a_2 T^2 + a_3 T^3 \tag{12}$$

where T = kelvin temperature, and the coefficients obtained are given in Table II. The standard deviation of the difference between the values obtained from Eq. (12) and the literature data is $\pm 0.4\%$ and the average

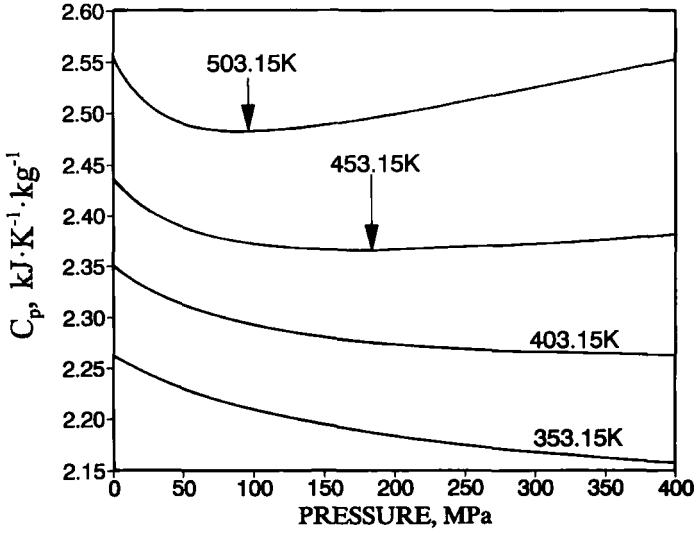

Fig. 4. Isobaric specific heat capacity of liquid *m*-cresol calculated with Eqs. (11) and (12). Vertical arrow points indicate minima.

Table VI. Isochoric Specific Heat Capacity of Liquid *m*-Cresol as $kJ \cdot K^{-1} \cdot kg^{-1}$

	T(K)			
p (MPa)	353.15	403.15	453.15	503.15
p_s	1.888	1.940	1.997	2.091
10.0	1.881	1.933	1.992	2.090
20.0	1.876	1.927	1.988	2.091
30.0	1.871	1.923	1.986	2.094
40.0	1.867	1.920	1.986	2.098
50.0	1.863	1.918	1.986	2.103
60.0	1.860	1.916	1.987	2.108
70.0	1.857	1.914	1.988	2.113
80.0	1.855	1.913	1.989	2.119
90.0	1.853	1.913	1.991	2.124
100.0	1.851	1.912	1.993	2.130
110.0	1.849	1.912	1.995	2.136
120.0	1.848	1.912	1.998	2.142
130.0	1.846	1.912	2.000	2.147
140.0	1.845	1.912	2.003	2.153
150.0	1.844	1.913	2.005	2.158
160.0	1.843	1.913	2.008	2.164
170.0	1.842	1.914	2.010	2.169
180.0	1.842	1.914	2.013	2.175
190.0	1.841	1.915	2.016	2.180
200.0	1.840	1.916	2.018	2.185
210.0	1.840	1.916	2.021	2.191
220.0	1.839	1.917	2.024	2.196
230.0	1.839	1.918	2.026	2.201
240.0	1.839	1.919	2.029	2.206
250.0	1.838	1.920	2.032	2.211
260.0	1.838	1.921	2.034	2.215
270.0	1.838	1.922	2.037	2.220
280.0	1.837	1.923	2.039	2.225
290.0	1.837	1.924	2.042	2.230
300.0	1.837	1.925	2.045	2.234
310.0	1.837	1.926	2.047	2.239
320.0	1.837	1.927	2.050	2.243
330.0	1.837	1.928	2.052	2.248
340.0	1.837	1.929	2.055	2.252
350.0	1.837	1.930	2.057	2.256
360.0	1.837	1.931	2.060	2.261
370.0	1.837	1.932	2.062	2.265
380.0	1.837	1.933	2.065	2.269
390.0	1.837	1.934	2.067	2.273
400.0	1.837	1.935	2.069	2.277

difference is +0.25%. The isobaric heat capacities derived with Eqs. (11) and (12) for pressures up to 400 MPa and at 353.15, 403.15, 453.15, and 503.15 K are given in Fig. 4.

3.6. Isochoric Heat Capacity, C_v^l

The isochoric heat capacity of liquid *m*-cresol at selected temperatures as a function of pressure up to 400 MPa was calculated with Eq. (13),

$$C_v^l = C_p^l - Tv\alpha_p^2/\kappa_T \tag{13}$$

Values for C_p^l were derived from data in Table V and Eqs. (11) and (12); values for v were from Table III as calculated with Eqs. (5) and (6); values for α_p were calculated with Eqs. (2)–(4); and values for κ_T, with Eq. (8). The resulting values of C_v^l are presented in Table VI.

3.7. Error Analysis

Estimation of the accuracy of the computed values presented in this paper is made difficult by the necessary sequences of fitting, integrating, and differentiating. Thus, an empirical approach has been taken by determining the effect on the calculated values of shifting the input experimental data by a fixed percentage. The results show that the error in the calculated value is proportional to the error in the input data, i.e., there is no significant error amplification by the calculation procedures used in this study [23]. The estimated uncertainties in the data in Tables III, V, and VI are indicated by the number of significant digits listed.

4. DISCUSSION

In the absence of a quantitative theory for dense molecular fluids, description of experimental data for liquids over large pressure and temperature ranges must be done by direct comparison of data for different liquids. Data for *m*-cresol, a self-associated liquid at room temperature and pressure, can be compared to a liquid such as *n*-hexane, without strong intermolecular interactions, and to a liquid with strong intermolecular interactions, such as water.

One of the more interesting observations for dense liquids without strong intermolecular interactions is the existence of a unique crossing point in isotherms of isobaric thermal expansivity [17]. The existence of such a point means that there is a pressure (usually below 100 MPa, e.g., 65 ± 2 MPa for *n*-hexane), where the isobaric thermal expansivity is independent of temperature. There is no unique crossing point in isotherms of

isobaric thermal expansivities for *m*-cresol (Fig. 1). The isotherms do cross near 100 MPa, but the crossing points are temperature dependent. The isotherms cross at lower pressures as temperature increases (see Fig. 1). A unique crossing point may exist at some high temperature where *m*-cresol is unassociated, since the low-temperature behavior probably results from the association equilibrium.

Self-association also affects the pressure effects on the heat capacities. $\Delta_{p_s}^{p} C_{p,T}^{l}(p)$ values for *m*-cresol at four temperatures are given in Fig. 5, and for comparison, $\Delta_{p_s}^{p} C_{p,T}^{l}(p)$ values for *n*-hexane [1] are given in Fig. 6. In the case of *n*-hexane, the isotherms of $\Delta_{p_s}^{p} C_{p,T}^{l}(p)$ do not cross but do show a minimum. The minimum shifts to higher pressures and the absolute values of $\Delta_{p_s}^{p} C_{p,T}^{l}(p)$ increase as temperature increases. For *m*-cresol, the minimum shifts to lower pressures and the absolute values of $\Delta_{p_s}^{p} C_{p,T}^{l}(p)$ below the crossing point decrease as the temperature increases; the opposite of the trends shown by *n*-hexane. Although no minimum is shown in the isotherms at 353 and 403 K for *m*-cresol, such a minimum is expected at higher pressures.

The behavior of *m*-cresol can be explained by pressure and temperature dependent self-association equilibria. At $T \geqslant 453$ K the hydrogen bonds are mostly broken and *m*-cresol behaves like a liquid without strong intermolecular interactions. At lower temperatures, where hydrogen bonding is significant, increasing pressure shifts the equilibrium toward the state with lower volume. At low temperatures both the shift in hydrogen-bonded equilibria and the contribution from weak intermolecular interactions contribute to the pressure effect on C_p^l. Detailed discussion of these interactions is beyond the scope of this study, however.

Accurate data are available for water as another example of a hydrogen-bonded liquid. Figure 7 presents the results of calculations of the isobaric heat capacity of liquid water from literature data [24]. There are strong similarities between the pressure effects on the heat capacity of *m*-cresol and of water. In both liquids, the pressure effect decreases as the temperature increases, and the isotherms of $\Delta_{p_s}^{p} C_{p,T}^{l}(p)$ at different temperatures diverge, converge, cross at different points, and then diverge again as the pressure increases. In liquids without strong intermolecular interactions such as *n*-hexane, isotherms of $\Delta_{p_s}^{p} C_{p,T}^{l}(p)$ at different temperatures diverge throughout the pressure range studied (see Fig. 5).

Comparison of the behavior of isobaric and isochoric heat capacities of *m*-cresol with increasing pressure and temperature is also informative. At 353.15 K the isochoric heat capacity decreases or is constant with increasing pressure up to 400 MPa (see Fig. 8 and Table VI). With increasing temperature, the isotherms exhibit a minimum that shifts to lower pressures. Similar effects occur in isotherms of the isobaric heat

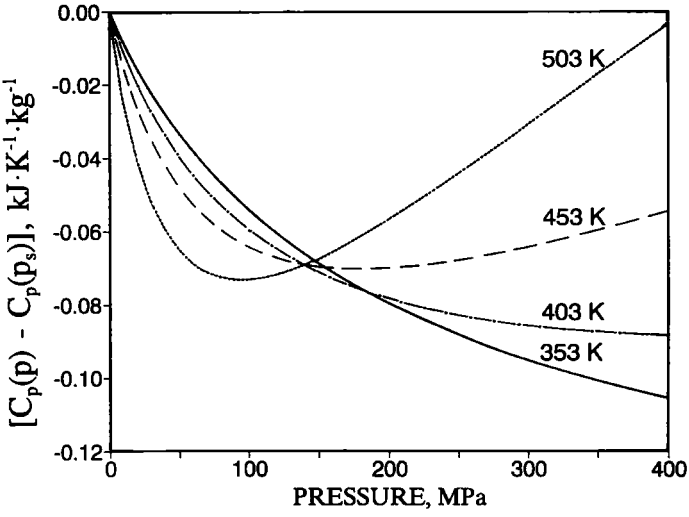

Fig. 5. Isothermal pressure increments of isobaric heat capacity of liquid *m*-cresol calculated with Eq. (10).

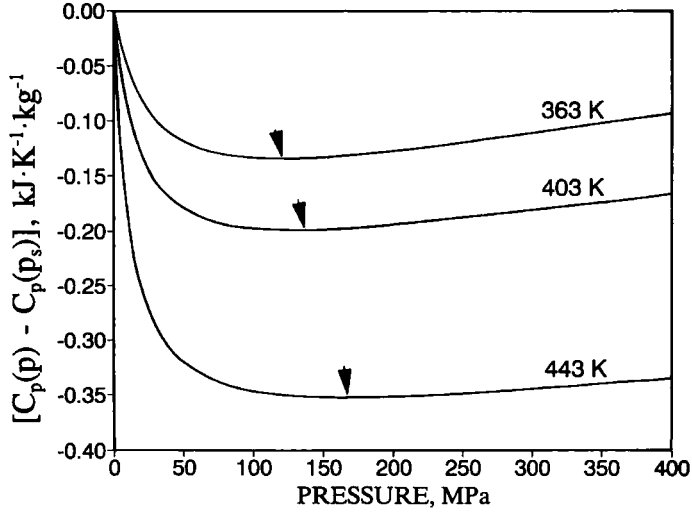

Fig. 6. Isothermal pressure increments of isobaric heat capacity of *n*-hexane as a function of pessure [1]. Arrows indicate minima.

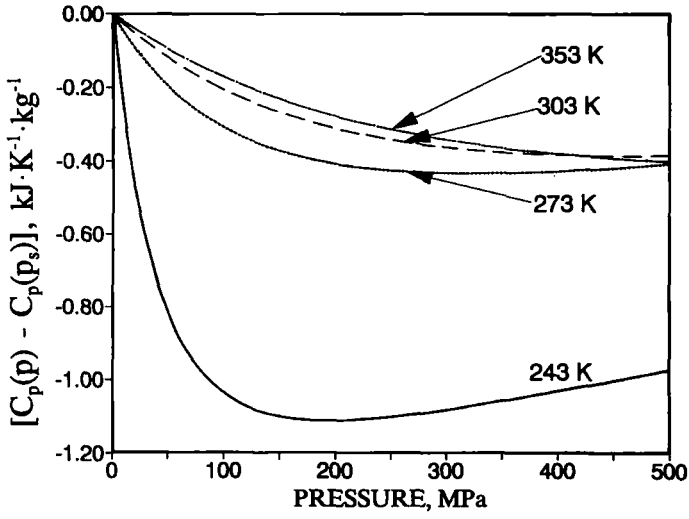

Fig. 7. Isothermal pressure increments of isobaric heat capacity of liquid water (supercooled at 243 K) as a function of pressure [24].

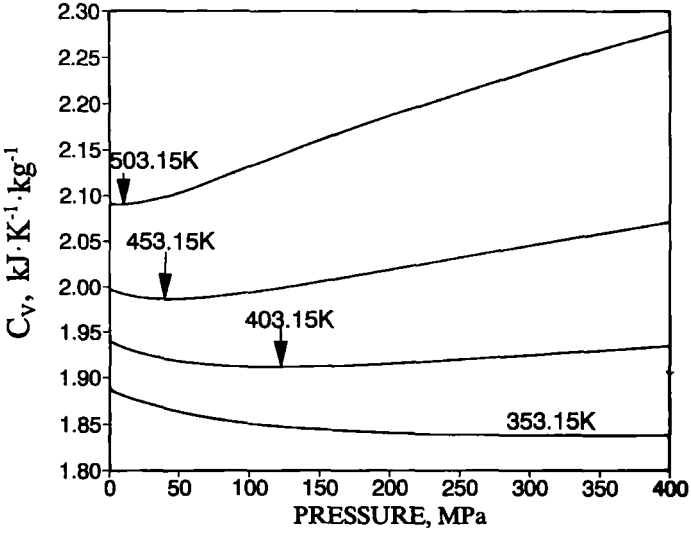

Fig. 8. Isochoric specific heat capacity of liquid *m*-cresol calculated with Eq. (13). Vertical arrow points indicate minima.

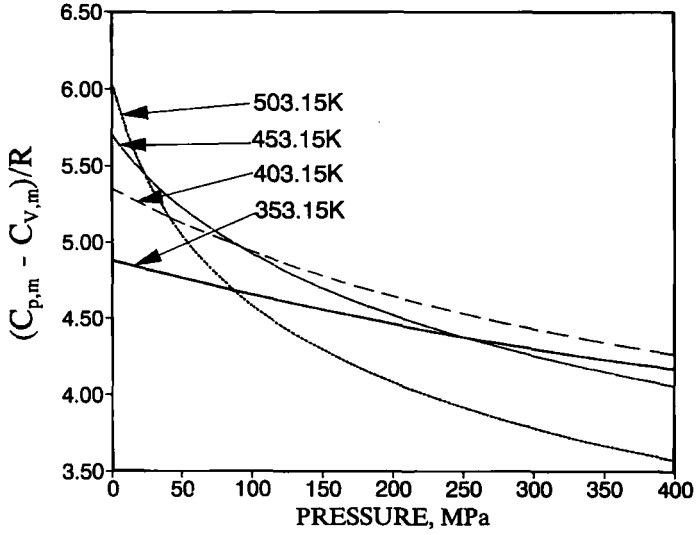

Fig. 9. Isotherms of the difference between isobaric and isochoric molar heat capacities of liquid *m*-cresol.

capacity (Fig. 4). The isotherms of the difference in the molar heat capacities, i.e., $C^{l}_{p,m} - C^{l}_{v,m}$, for *m*-cresol (Fig. 9) do not show the regular behavior observed for liquids without strong molecular interaction. In the case of *n*-hexane, isotherms of $C^{l}_{p,m} - C^{l}_{v,m}$ all converge to a value of 5R at 20 MPa, above which they are continuously divergent. The only regularities apparent in the isotherms for *m*-cresol are an increase in the value with temperature at atmospheric pressure and an increasingly negative pressure derivative with increasing temperature.

In conclusion, this study provides a set of data that can be used to test predictions of associated liquid models over wide ranges of temperature and pressure.

ACKNOWLEDGMENT

S.L.R. wishes to express appreciation for the hospitality and financial support received from the Department of Chemistry, Brigham Young University, during his visits there.

REFERENCES

1. S. L. Randzio, J.-P. E. Grolier, J. R. Quint, D. J. Eatough, E. A. Lewis, and L. D. Hansen, *Int. J. Thermophys.* 15:415 (1994).
2. E. M. Woolley, J. G. Travers, B. O. Erno, and L. G. Hepler, *J. Phys. Chem.* 76:3591 (1971).

3. J. N. Spencer, C. L. Campanella, E. M. Harris, and W. S. Wolbach, *J. Phys. Chem.* **89**:1888 (1985),
4. J. N. Spencer, J. A. Andrefsky, J. Naghdi, L. Patti, and J. F. Tarder, *J. Phys. Chem.* **91**:2959 (1987).
5. J. N. Spencer, K. N. Allot, S. Chanandin, B. G. Enders, A. Grushow, S. P. Kneizys, D. Mobley, J. Naghdi, L. M. Patti, and J. S. Salata, *J. Solut. Chem.* **17**:287 (1988).
6. C. M. White, F. K. Schweighardt, and J. Shultz, *Fuel Process. Technol.* **1**:209 (1978).
7. C. M. White and N. C. Li, *Anal. Chem.* **54**:1570 (1982).
8. C. M. White, L. Jones, and N. C. Li, *Fuel* **62**:1397 (1983).
9. G. D. Mohr, M. Mohr, A. J. Kidnay, and V. F. Yesavage, *J. Chem. Thermodyn.* **15**:425 (1983).
10. D. J. Eatough, S. L. Wolfley, L. J. Dungan, E. A. Lewis, and L. D. Hansen, *J. Energy Fuels* **1**:94 (1987).
11. A. Oikawa and M. Ito, *J. Mol. Spectrosc.* **126**:133 (1985).
12. H. Mizuno, K. Okuyama, T. Ebata, and M. Ito, *J. Phys. Chem.* **91**:5589 (1987).
13. S. L. Randzio, D. J. Eatough, E. A. Lewis, and L. D. Hansen, *J. Chem. Thermodyn.* **20**:937 (1988).
14. L. Ter Minassian and Ph. Pruzan, *J. Chem. Thermodyn.* **9**:375 (1977).
15. S. L. Randzio and J. Zaslona, Polish Patent 285871.
16. S. L. Randzio, J.-P. E. Grolier, and J. R. Quint, *Rev. Sci. Instrum.* **65**:960 (1994).
17. S. L. Randzio, *Phys. Lett. A* **117**:1473 (1986).
18. K. F. Goldblum, R. W. Martin, and R. B. Young, *Ind. Eng. Chem.* **39**:1471 (1947).
19. P. Nasir, S. C. Hwang, and R. Kobayashi, *J. Chem. Eng. Data* **25**:298 (1980).
20. D. H. Krevor, F. W. Lam, and J. M. Prausnitz, *J. Chem. Eng. Data* **31**:353 (1986).
21. V. G. Niesen and V. F. Yesavage, *J. Chem. Eng. Data* **33**:138 (1988).
22. TRC Thermodynamic Tables, *Nonhydrocarbons* **8**:Vc-640.
23. S. L. Randzio, J.-P. E. Grolier, and J. R. Quint, *Fluid Phase Equil.* (in press).
24. L. Ter Minassian, Ph. Pruzan, and A. Soulard, *J. Chem. Phys.* **75**:3064 (1981).